



Influence of Nano Silica Particles on Quasistatic Mechanical and Low Velocity Impact Properties of Carbon-Glass-Sunn Hemp/Epoxy in Intra-Inter Ply Hybrid Composites

M Bharathi¹, S Senthil Kumaran², P Edwin Samson²

¹Central Institute of Plastics Engineering and Technology, Chennai, Tamilnadu, India

²Department of Mechanical Engineering, Anna University, Chennai, Tamilnadu, India

Email: m.bharathi1219@gmail.com

Article History

Received: 2 June 2021

Accepted: 8 May 2022

Keywords:

Flexural;
Compression;
ILSS;
LVI;
damage assessment;
eco-friendly composites;
intra-interply hybrid composites

Abstract

Increasing fuel prices and emission norms have favoured the automobile manufactures to use of lightweight materials. Land fill regulations imposed by many environmental governing agencies encourage the use of products which will decompose easily or which will require lesser energy for recycling. In this scenario an attempt has been made in this work to develop natural fiber hybrid composites with natural and synthetic fibers to address the issue of harm to the environment and energy spent on recycling. In this work the flexural, compression, interlaminar shear stress and low velocity impact properties of natural fiber hybrid composite reinforced with carbon +E-glass intra plies, unidirectional sunn hemp mat interplies and nano silica particles are investigated for possible application in automobiles. It is found that the addition of nano silica particles enhances the flexural, compression, interlaminar shear strength and low velocity impact properties of the composite.

1. Introduction

Increasing fuel prices and emission norms have favored the automobile manufactures the use of lightweight materials (Akampumuza et al. Zah et al.). Composites are lighter in weight and are widely used in automobile, aerospace industries (Santini et al. Ramu, Kumar, and Palanikumar). While composites offer many advantages, the recycling of outdated composite materials is a serious issue. Land fill regulations imposed by many environmental governing agencies encourage the use of products which will decompose easily or which will require lesser energy for recycling (Das et al.). In this scenario an attempt has been made in this work to develop natural fiber hybrid composites with natural and synthetic fibers to address the issue of

harm to the environment and energy spent on recycling (Mohan and Kanny Reddy et al.). Several automobiles manufactures and their association are aiming to incorporate plant-based materials in their future vehicles. Developing natural fiber hybrid composite with reduced quantum of synthetic fibers will be of immense use to the automobile manufactures as the natural fibers are light weighted and ecofriendly. Natural fiber hybrid composite is a composite blend that is reinforced with natural fibers and synthetic fibers that incorporates the advantages of both synthetic and natural fibers (Manral, Ahmad, and Chaudhary). Natural fibres in natural fibre hybrid composites help to improve impact load bearing qualities and recycling difficulties.

Composites reinforced with carbon fiber are

pricey and have higher strength to weight ratio and are limited to exotic applications such as race cars. Compared to carbon fibers, E-glass fibers have higher failure strain and comparatively lower in cost. Hybridization of carbon fibers with E-glass fibers blends the benefit of both the fibers, paving the way for growth of economical composites. Jute, sisal, hemp, flax is some of the natural fibers used for reinforcement in a composite (Sivakandhan et al.). Generally, the density of the natural fibers is lesser (Sair et al.). Among the natural fibers Sunn hemp fibers possess strength equivalent to that of E-glass and possess good impact load bearing characteristics.

Ashok Raj purohit et al. (2020) have found out that the presence of E-glass fibers in Carbon +E-glass intrapplies reduces the evolution of cracks in the carbon fibers, when the carbon+E-glass intrapplies are subjected to load (Rajpurohit et al.). Zhang et.al (2012) have found that that improvement in the failure strain by hybridizing carbon, E-glass fibers (J. Zhang et al.). They have found out that the tensile properties of intraply carbon/carbon composites are higher when compared with interply composites (Ren and Z. Zhang). Authors have found that the load transferring characteristics between the fibers in an intraply composite is better than an interply composite. (Uzay, Acer, and Geren Pegoretti et al.) From the literature survey conducted, it has been found that only few research works are done in the area composites containing carbon fibres in the weft direction and E-glass fibres in the warp direction along with natural fibres as reinforcing elements.

The goal of this research is to analyse the flexural, compression, interlaminar shear stress, and low velocity impact properties of a natural fibre hybrid composite reinforced with plies containing carbon fibres in the weft direction and E-glass fibres in the warp direction, parallel oriented sunn hemp fibre mats, and $40 \mu \text{SiO}_2$ particles for use in automobiles.

2. Material Selection and Fabrication of Composites

In this study, plies containing carbon fibres present in both weft direction and warp direction, plies containing E-glass fibres present in the weft direction and warp direction, plies with carbon fibres present in the weft direction and E-glass fibres in the warp direction, parallel oriented woven sunn hemp mats, and $40 \mu \text{SiO}_2$ particles were employed as reinforcing

materials. Each filament in the synthetic fibres were of 3000 Tex and the matrix was made of epoxy and hardener (10:1 weight ratio). The orientation of the various mats in the composites is shown in the Figure 1 (a-g). Composite laminates were made by hand layup technique and subsequently pressed in a press. Composite panels of size 300mm in length and 300 mm in width were fabricated which is then post-cured for 24 hours at ambient temperature.

Test coupons based on ASTM standards were precisely cut from the composite panel. While preparing the specimens from Fibre-Reinforced Polymer 2 (FRP 2) composites, it was ensured that the filaments of carbon fibres, E-glass fibres and parallel oriented sunn hemp mats were aligned along the direction of load. While preparing the composites from Fibre-Reinforced Polymer 3 (FRP 3) to Fibre-Reinforced Polymer 7 (FRP 7) composites, it was also ensured that carbon fibres and parallel oriented sunn hemp fibres were aligned along the direction of load.

2.1. Arrangement of various plies in the Composites

Seven distinct composites were fabricated and the arrangement of various mats in the composite is shown in the Figure 1(a-g).

In addition to carbon fibres, E-glass fibres and parallel oriented sunn hemp mats, the composites Fibre-Reinforced Polymer 4 (FRP 4), Fibre-Reinforced Polymer 5 (FRP 5), Fibre-Reinforced Polymer 6 (FRP 6), Fibre-Reinforced Polymer 7 (FRP 7) were further reinforced with $40 \mu \text{SiO}_2$ particles in 1 weight %, 2 weight %, 3 weight %, and 4 weight % respectively.

Fibre-Reinforced Polymer 1 (FRP 1) Parallel oriented Sunn Hemp mat

Fibre-Reinforced Polymer 2 (FRP 2) Carbon fibre, E-glass fibre and Parallel oriented Sunnhemp

Fibre-Reinforced Polymer 3 (FRP 3) Plies with carbon fibres present in the weft direction and E-glass fibres in the warp direction and Parallel oriented Sunnhemp

Fibre-Reinforced Polymer 4 (FRP 4) Plies with carbon fibres present in the weft direction and E-glass fibres in the warp direction and Parallel oriented Sunnhemp with 1weight % $40 \mu \text{SiO}_2$

Fibre-Reinforced Polymer 5 (FRP 5) Plies with carbon fibres present in the weft direction and E-

glass fibres in the warp direction and Parallel oriented Sunnhemp with 2% weight 40 μ SiO₂

Fibre-Reinforced Polymer 6 (FRP 6) Plies with carbon fibres present in the weft direction and E-glass fibres in the warp direction and Parallel oriented Sunnhemp with 3% weight 40 μ SiO₂

Fibre-Reinforced Polymer 7 (FRP 7) Plies with carbon fibres present in the weft direction and E-glass fibres in the warp direction and Parallel oriented Sunnhemp with 4% weight 40 μ SiO₂

3. Experimental Details

3.1. Flexural Test

The flexural test was done with an UTM (Instron make model number 3382). The test was done by following ASTM D790 standard. Standard test coupons of dimension 127 x 12.7 mm were machined for the conduct of flexural test.

3.2. Compression Test

The compression test was done with an UTM (Instron make model number 3382). The test was done by following ASTM D3410 standard. Standard test coupons of dimension 250 x 20 mm were machined for the conduct of compression test.

3.3. Interlaminar Shear Strength Test (ILSS)

The ILSS test was conducted with an UTM (Instron make model number 3382). The test was done by following ASTM D2344 standard. Standard test coupons of dimension 60 x 12.7 mm were machined for the conduct of ILSS test.

3.4. Low Velocity Impact Test (LVI)

The low velocity impact test was carried on the specimens of dimensions 90 x 90 mm as per ASTM D5628 standard by using Fractovis Plus drop mass setup and is shown in the Figure1(d). A rigid hemispherical steel impactor of radius 6.35 mm with a mass of 1.92 kg was utilized for impacting the clamped specimens at a velocity of 3m/s and the low velocity impact characteristics were studied.

According to (Tita, de Carvalho, and Vandepitte) the impact energy on the composite during a low velocity impact event is partially absorbed by the composite as permanent damage in the composite and partially stored as elastic energy in the composite. The absorbed energy and elastic energy can be calculated from the Impact Energy Vs Time output characteristics of the LVI test. The absorbed

energy and elastic energy of the various composites were calculated from the output characteristics of low velocity impact test.

3.5. Damage Assessment

3.5.1. Scanning Electron Microscopic Analysis

The scanning electron microscopy was used to understand the failure mechanisms associated with the composites (Srinivasan et al. Wielage et al.). The fractured surface of the specimens failed in flexural, compression, ILSS tests were examined using Hitachi Make, Model Number HTAC 1 S -3400N is shown in Figure 3.1. The specimens were gold coated with an ion sputtering device in order to reduce sample charge and improve image contrast.

3.5.2. Digital Microscopy

Macroscopic analysis and damage assessment of the low velocity impacted specimens was carried out with a digital camera and Olympus make digital measuring microscope (STM7) with a 3 X measuring objective (shown in Figure 3). The image of the sample which was mounted on the xy-stage was captured using the integrated camera and damage assessment was made.

3.5.3. Image J software

Digital photographs of the low velocity impacted specimens were taken with a digital camera and imported to 'Image J software', a JAVA based image processing tool. After importing the digital photograph to the software, the dimension represented by a pixel in the image is calibrated and the damaged area is measured by drawing a line along the affected portions perimeter (Vasudevan et al. Dong).

4. Results and Discussion

4.1. Flexural properties

The results of the flexural test of the fabricated composites FRP 1, FRP 2 and FRP 3 are shown in Figure 4 a & 4 b.

From Figure 4, it can be found that, Fibre-Reinforced Polymer 3 (FRP 3) displays a flexural strength of 306.41 MPa in the flexural test. This is higher than Fibre-Reinforced Polymer 2 (FRP 2) which possesses flexural strength of 300.71 MPa. The flexural strength of Fibre-Reinforced Polymer 3 (FRP 3) and Fibre-Reinforced Polymer 2 (FRP 2) differed by 5.7 MPa which is reasonably higher. The higher flexural value of Fibre-Reinforced Poly-

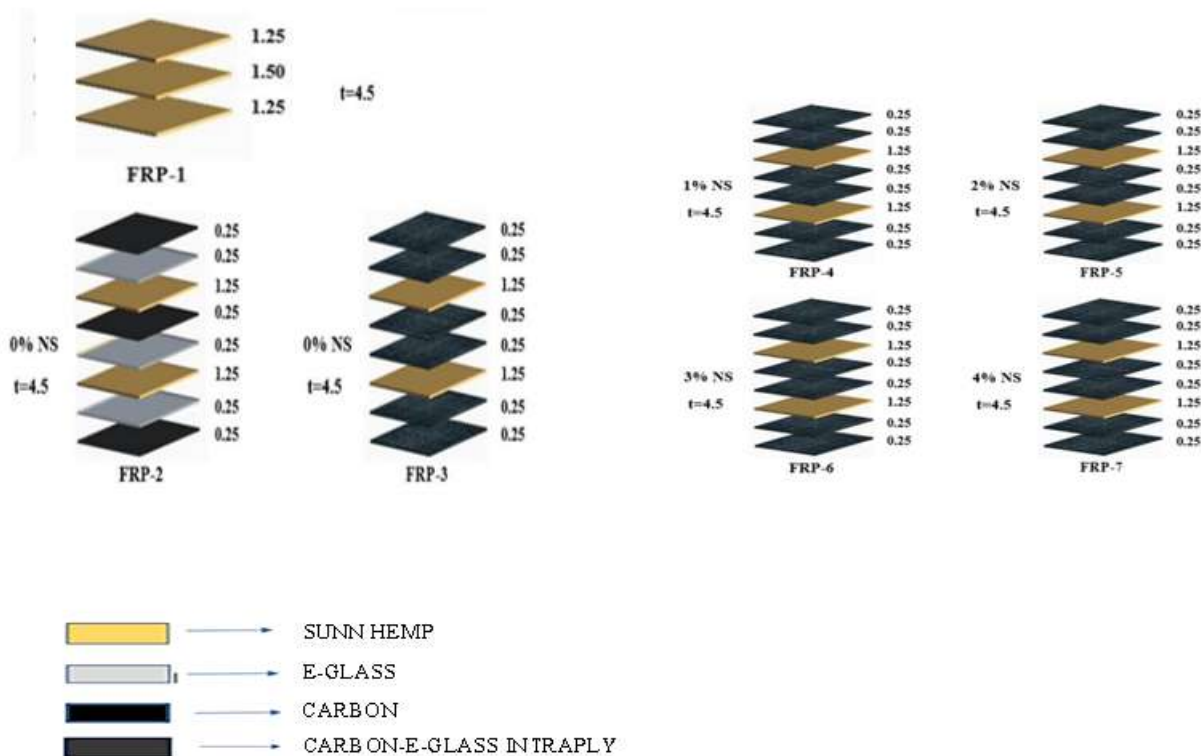


Figure 1. (a-g) FRP 1- a, FRP 2- b, FRP 3 - c, FRP 4 – d, FRP 5 – e, FRP 6 – f, FRP 7 - g

FIGURE 1. (a-g) Arrangement of various plies in the composites

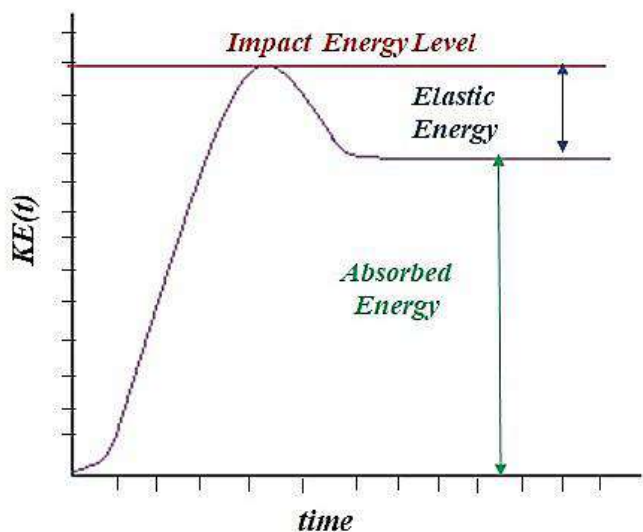


FIGURE 2. Impact Energy Vs Time

mer 3 (FRP 3) can be ascribed to the better load transfer between superior strength carbon fibres and relatively ductile E-glass fibres present in the same stack. Presence of E-glass fibres in plies with car-



FIGURE 3. (a) Scanning Electron Microscope & (b) Digital Measuring Microscope

bon fibres present in the weft direction and E-glass fibres in the warp direction also lessens the concentration of cracks which could evolve in carbon fibres under load. This additionally helps in better load bearing characteristics due to the intraply arrangement of carbon fibres and E-glass fibres present in the same ply. In the Fibre-Reinforced Polymer 3 (FRP 3) composite, synergistically along with the carbon, E-glass fibres, parallel oriented sunn hemp

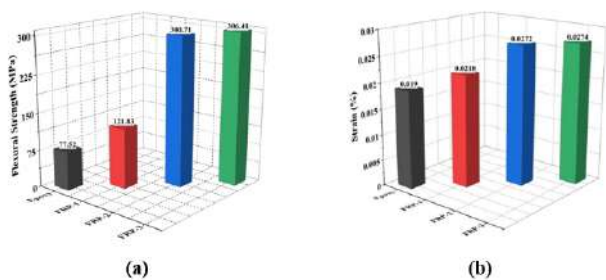


FIGURE 4. (a) Flexural strength of Fibre-Reinforced Polymer 1 (FRP 1), Fibre-Reinforced Polymer 2 (FRP 2), Fibre-Reinforced Polymer 3 (FRP 3) composites (b) Flexural strain of Fibre-Reinforced Polymer 1 (FRP 1), Fibre-Reinforced Polymer 2 (FRP 2), Fibre-Reinforced Polymer 3 (FRP 3) composites

fibres have approximately shared 39.7 % of the flexural load. From Figure 4 (b) it can be inferred that the flexural strain of Fibre-Reinforced Polymer 3 (FRP 3) is 0.0274 % and Fibre-Reinforced Polymer 2 (FRP 2) is 0.0272 %. Both the composites considered in the study doesn't exhibit much flexural strain. The lower failure strain of the composites can be ascribed to the failure of the thermoset matrix utilized in the composites.

4.2. Compressive Properties

The compressive test results of the various composites considered in the study is shown in Figure 5 (a) and Figure 5 (b).

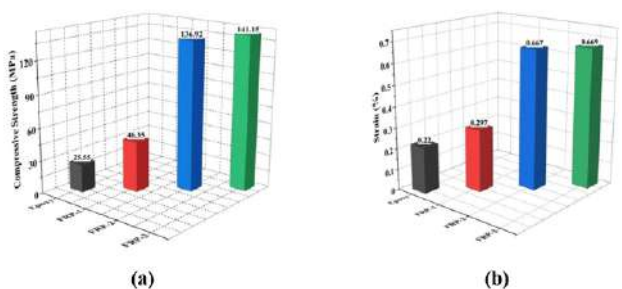


FIGURE 5. (a) Compressive strength of Fibre-Reinforced Polymer 1 (FRP 1), Fibre-Reinforced Polymer 2 (FRP 2), Fibre-Reinforced Polymer 3 (FRP 3) composites (b) Compressive strain of Fibre-Reinforced Polymer 1 (FRP 1), Fibre-Reinforced Polymer 2 (FRP 2) and Fibre-Reinforced Polymer 3 (FRP 3) composites

From Figure 5, it can be found that, Fibre-Reinforced Polymer 3 (FRP 3) displays a compressive strength of 141.15 MPa in the compressive

test. It is reasonably higher than 136.92 Mpa, the compressive strength exhibited by Fibre-Reinforced Polymer 2 (FRP 2). The compressive strength exhibited by Fibre-Reinforced Polymer 3 (FRP 3) and Fibre-Reinforced Polymer 2 (FRP 2) differ by 4.2 MPa, which is reasonably higher. The presence of superior strength carbon fibres and relatively ductile E-glass present in the same stack in the weft and warp directions increases the compressive strength of Fibre-Reinforced Polymer 3 (FRP 3). This additionally results in better load carrying characteristics. Further in Fibre-Reinforced Polymer 3 (FRP 3) composites, the presence of larger amount of carbon fibres in the loading direction enhances the load bearing capabilities. In the Fibre-Reinforced Polymer 3 (FRP 3) composites, synergistically along with the carbon fibre, E-glass fibres, parallel oriented sunn hemp fibres have shared approximately 32 % of the compressive load. From Figure 5 b it can be inferred that the compressive strain of Fibre-Reinforced Polymer 3 (FRP 3) is 0.669 % and Fibre-Reinforced Polymer (FRP 2) is 0.667 %. Both the composites considered in the study doesn't exhibits higher compressive strain. The lower failure strain of the composites may be ascribed to the failure of the matrix utilized in the composites.

4.3. Interlaminar Shear Strength

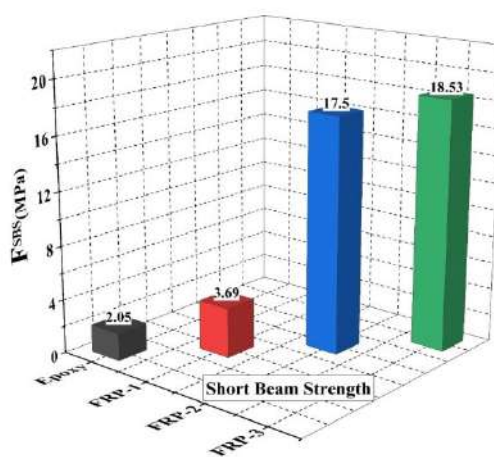


FIGURE 6. Interlaminar Shear strength of Fibre-Reinforced Polymer 1 (FRP 1), Fibre-Reinforced Polymer 2 (FRP 2), Fibre-Reinforced Polymer 3 (FRP 3) composites

The ILSS test results of the composites Fibre-Reinforced Polymer 1 (FRP 1), Fibre-Reinforced Polymer 2 (FRP 2), Fibre-Reinforced Polymer 3

(FRP 3) considered in the study is shown in Figure 6. From Figure 6, it can be found that the interlaminar shear strength (short beam test) of Fibre-Reinforced Polymer 3 (FRP 3) composite is 18.5 MPa. It is inferred from the results that ILSS of Fibre-Reinforced Polymer 3 (FRP 3) value is slightly higher than ILSS of Fibre-Reinforced Polymer 2 (FRP 2). The difference in interlaminar shear strength between Fibre-Reinforced Polymer 3 (FRP 3) and Fibre-Reinforced Polymer 2 (FRP 2) can be attributed to the matrix failure in the composite.

5. Effect of Addition of $40 \mu \text{SiO}_2$ Particles on the Flexural, Compression, Interlaminar Shear Stress and Low Velocity Impact Properties.

Based on the flexural, compression and interlaminar shear strength estimated for the Fibre-Reinforced Polymer 1 (FRP 1), Fibre-Reinforced Polymer 2 (FRP 2), Fibre-Reinforced Polymer 3 (FRP 3), the composites with better properties i.e. Fibre-Reinforced Polymer 3 (FRP 3) was further reinforced with varying levels of $40 \mu \text{SiO}_2$ particles (1 weight %, 2 weight %, 3 weight % and 4 weight %) and their flexural, compression, interlaminar shear stress and low velocity impact properties were investigated.

5.1. Flexural Properties of Composites reinforced with varying levels of $40 \mu \text{SiO}_2$ particles

The results of the flexural tests of Fibre-Reinforced Polymer 3 (FRP 3), Fibre-Reinforced Polymer 4 (FRP 4), Fibre-Reinforced Polymer 5 (FRP 5), Fibre-Reinforced Polymer 6 (FRP 6), Fibre-Reinforced Polymer 7 (FRP 7) are shown in the following Figure 7.

From Figure 7. it can be proved that the addition of $40 \mu \text{SiO}_2$ particles up to 3 weight % improves the flexural strength. When the incorporation of $40 \mu \text{SiO}_2$ particles increased further, it results in reduced flexural strength and it can be attributed to agglomeration of the $40 \mu \text{SiO}_2$ particles.

Further, from Figure 7. it can be identified that Fibre-Reinforced Polymer 6 (FRP 6) possesses a flexural strength of 348.18 MPa which is higher than the flexural strength 306.41 MPa exhibited by Fibre-Reinforced Polymer 3 (FRP 3). Fibre-Reinforced Polymer 6 (FRP 6) differs in the flexural strength from Fibre-Reinforced Polymer 3 (FRP 3) by 41.77 MPa. It is identified that by the addition $40 \mu \text{SiO}_2$ up to 3 weight % increases the flexural strength

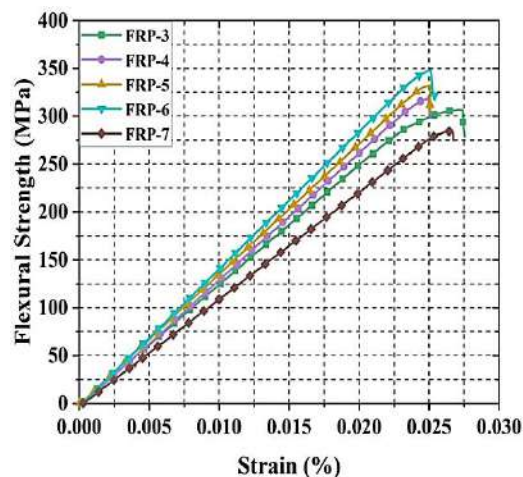


FIGURE 7. Flexural Strength Vs. Strain of Fibre-Reinforced Polymer 3 (FRP 3), Fibre-Reinforced Polymer 4 (FRP 4), Fibre-Reinforced Polymer 5 (FRP 5), Fibre-Reinforced Polymer 6 (FRP 6), Fibre-Reinforced Polymer 7 (FRP 7) composites

by 12 %. The enhanced flexural strength may be attributed to enhanced bonding between the matrix and the reinforced fibre by the addition of $40 \mu \text{SiO}_2$ particles. The increase in strength may be attributed to dispersion strengthening of the matrix by the addition of $40 \mu \text{SiO}_2$ particles. From the flexural test conducted on the various composites it can be stated that $40 \mu \text{SiO}_2$ particles plays a vital role to improve the flexural strength of the composites taken in the study.

Figure 7. reveals that the flexural strain of the composites doesn't differ much and it can be attributed to the failure of the matrix used in the composite. It can be stated that, the flexural strain is insignificant to the addition of $40 \mu \text{SiO}_2$ particle. The lower failure strain of the composites can be due to the failure of the thermoset matrix used in the composites.

5.2. Compressive Properties of composites reinforced with varying levels of $40 \mu \text{SiO}_2$ particles

The compressive properties of the composites Fibre-Reinforced Polymer 3 (FRP 3), Fibre-Reinforced Polymer 4 (FRP 4), Fibre-Reinforced Polymer 5 (FRP 5), Fibre-Reinforced Polymer 6 (FRP 6), Fibre-Reinforced Polymer 7 (FRP 7) are shown in the Figure 8.

The interlaminar shear strength of the composites

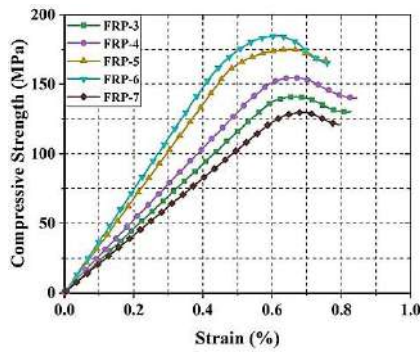


FIGURE 8. Compressive strength of Fibre-Reinforced Polymer 3 (FRP 3), Fibre-Reinforced Polymer 4 (FRP 4), Fibre-Reinforced Polymer 5 (FRP 5), Fibre-Reinforced Polymer 6 (FRP 6), Fibre-Reinforced Polymer 7 (FRP7) composites

FRP 3, FRP 4, FRP 5, FRP 6 and FRP 7 were estimated and the results are shown in the Figure 7.

From Figure 7. it can be proved that the addition of $40 \mu \text{SiO}_2$ particles up to 3 weight % improves the compressive strength. When, the addition of $40 \mu \text{SiO}_2$ particles increased further it results in reduced compressive strength decreases. It can be attributed to agglomeration effect of the $40 \mu \text{SiO}_2$ particles.

Further from Figure 7., it can be identified that, Fibre-Reinforced Polymer 6 (FRP 6) possesses a compressive strength of 184.76 MPa which is higher than Fibre-Reinforced Polymer 3 (FRP 3) which exhibits a compressive strength of 141.15 MPa. Fibre-Reinforced Polymer 6 (FRP 6) differs from Fibre-Reinforced Polymer 3 (FRP 3) in compressive strength by 43.61 MPa, which is also significant. It is inferred from the results that the compressive strength increases by 23.6 %, and the improvement in the compressive strength can be attributed to the incorporation of 3 weight % $40 \mu \text{SiO}_2$ particles. This enhancement in the compressive strength may be ascribed to increase in the bonding between the epoxy matrix and the reinforced fibres. The increase in strength may be attributed to dispersion strengthening of the matrix by the addition of $40 \mu \text{SiO}_2$ particles.

From Figure 7. it is inferred that the compressive strain of the composites doesn't differ much. The results reveals that the compressive strain is insignificant to the incorporation of $40 \mu \text{SiO}_2$ particles to the composites and the lower failure strain of the composites could be due the failure of the matrix in the composites.

5.3. Interlaminar Shear Strength of Composites reinforced with varying levels of $40 \mu \text{SiO}_2$ particles

Figure 9. reveals the results of the interlaminar shear strength of the composites Fibre-Reinforced Polymer 3 (FRP 3), Fibre-Reinforced Polymer 4 (FRP 4), Fibre-Reinforced Polymer 5 (FRP 5), Fibre-Reinforced Polymer 6 (FRP 6), Fibre-Reinforced Polymer 7 (FRP 7).

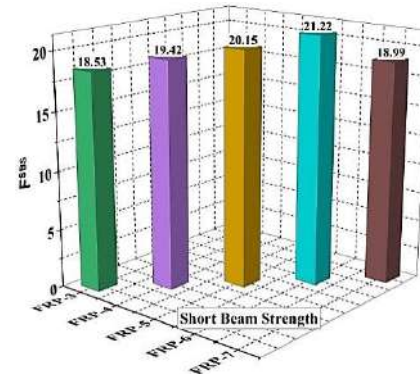


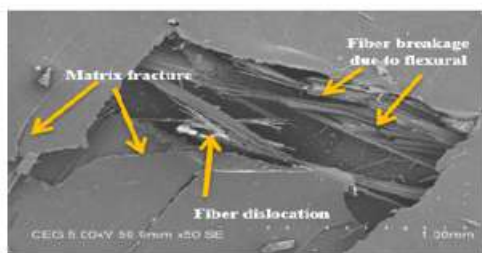
FIGURE 9. ILSS of Fibre-Reinforced Polymer 3 (FRP 3), Fibre-Reinforced Polymer 4 (FRP 4), Fibre-Reinforced Polymer 5 (FRP 5), Fibre-Reinforced Polymer 6 (FRP 6), Fibre-Reinforced Polymer 7 (FRP 7) composites.

Figure 9., reveals the interlaminar shear strength of Fibre-Reinforced Polymer 6 (FRP 6) is 21.22 MPa. It is found that Fibre-Reinforced Polymer 6 (FRP 6) value is higher than Fibre-Reinforced Polymer 3 (FRP 3) which possess interlaminar shear strength of 18.53 MPa.

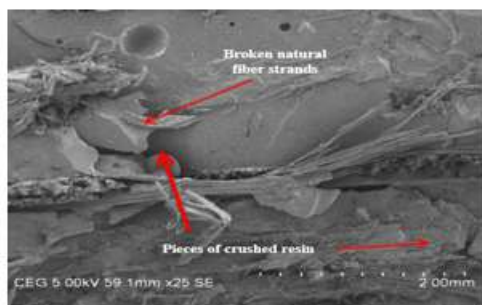
Interlaminar shear strength of Fibre-Reinforced Polymer 6 (FRP 6) differs from interlaminar shear strength of Fibre-Reinforced Polymer 3 (FRP 3) composite by 2.69 MPa, and it is marginally higher. Based on the results, the marginal improvement in interlaminar shear strength can be attributed to the dispersion strengthening of the epoxy matrix. It is also due to better fibre matrix bonding due to the addition of $40 \mu \text{SiO}_2$ particles.

5.4. Failure analysis of composites reinforced with varying levels of $40 \mu \text{SiO}_2$ particles.

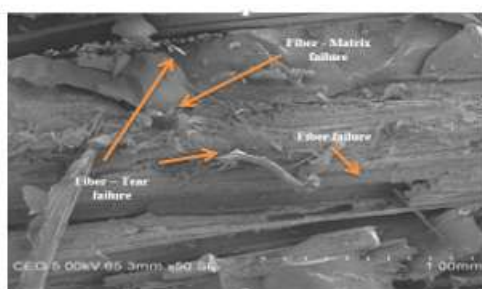
The results of the failure analysis of the Fibre-Reinforced Polymer 6 (FRP 6) composites failed in flexural, compression and ILSS tests by scanning electron microscopic analysis is shown in the Figures 10 (a-c)



(a)



(b)



(c)

FIGURE 10. SEM results of Fibre-Reinforced Polymer 6 (FRP 6) failed in (a) Flexural (b) Compression and (c) ILSS tests

The SEM analysis conducted on the specimen Fibre-Reinforced Polymer 6 (FRP 6) composite failed in flexural load reveals matrix fracture, fibre dislocation and fibre breakage. The SEM images of Fibre-Reinforced Polymer 6 (FRP 6) composite failed in compression test reveals broken natural fibre strands and pieces of crushed resin. The SEM images of Fibre-Reinforced Polymer 6 (FRP 6) composite failed in ILSS test reveals the various types of failures like fibre -matrix failure, fibre-tear failure and failure of the fibres.

6. Statistical Analysis of the Flexural, Compressive and Interlaminar Shear strength of the 40 μ SiO₂ reinforced composites

The analysis of the flexural, compressive and interlaminar shear strength properties of the 40 μ SiO₂ reinforced composites was carried out with analysis of variance (ANOVA) technique. Higher value of F and lower value of P are necessary for an effect to be statistically significant. The one-way analysis carried out for the properties of the various 40 μ SiO₂ reinforced composites is shown in Figures 11, 12 and 13.

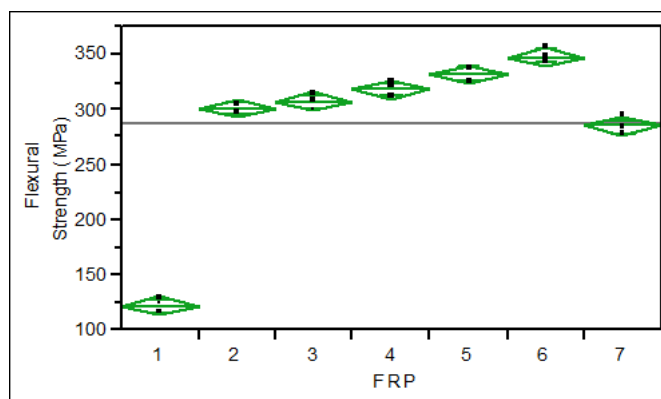


FIGURE 11. One-way Analysis of Flexural Strength (MPa) by FRP

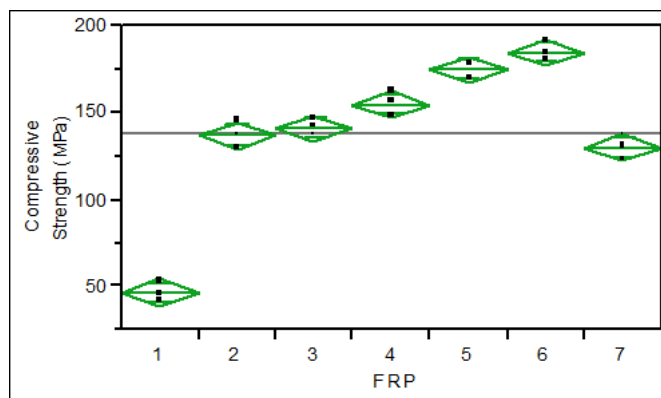


FIGURE 12. One-way Analysis of Compressive Strength (MPa) by FRP

Lower P values are observed for the flexural strength, compressive strength and interlaminar shear strength in the One-way ANOVA conducted. This statistically confirms the addition of 40 μ SiO₂ particle has profound influence on the above properties.

TABLE 1. Analysis of Variance for One-way Analysis of Flexural Strength (MPa) by FRP

Source	DF	Sum of Squares	Mean Square	F Ratio	Prob > F
F R P	6	103828.41	17304.7	387.2919	<.0001
Error	14	625.54	44.7		
C. Total	20	104453.95			

TABLE 2. Analysis of Variance for One-way Analysis of Compressive Strength (MPa) by FRP

Source	DF	Sum of Squares	Mean Square	F Ratio	Prob > F
F R P	6	36950.458	6158.41	156.0207	<.0001
Error	14	552.605	39.47		
C. Total	20	37503.063			

TABLE 3. Analysis of Variance for One-way Analysis of Short Beam Strength (MPa) by FRP

Source	DF	Sum of Squares	Mean Square	F Ratio	Prob > F
F R P	6	639.38010	106.563	34.8194	<.0001
Error	14	42.84640	3.060		
C. Total	20	682.22650			

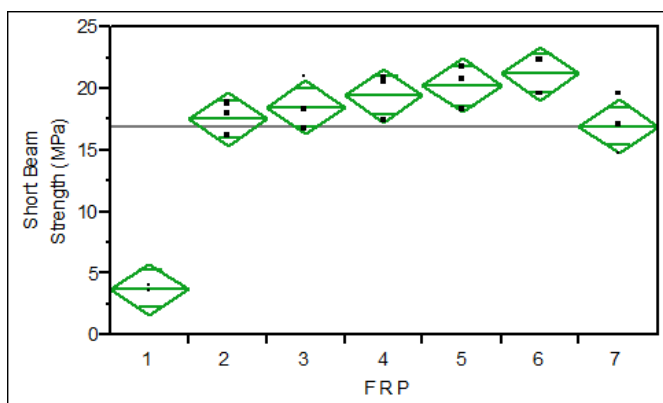


FIGURE 13. One-way Analysis of Short Beam Strength (MPa) by FRP

7. Low Velocity Impact Test

The various observations made during the low velocity impact test for the Fibre-Reinforced Polymer 3 (FRP 3), Fibre-Reinforced Polymer 4 (FRP 4), Fibre-Reinforced Polymer 5 (FRP 5), Fibre-Reinforced Polymer 6 (FRP 6) is shown in the Figure 15 (a-e) and Tabular column 1,2,3 and 4. As the flexural, compression and ILSS properties of Fibre-Reinforced Polymer 7 (FRP 7) was inferior, low velocity impact test of Fibre-Reinforced Polymer 7 (FRP 7) was not carried out.

From Figure 14 (b) it can be identified that there is an increase in the peak force of Fibre-Reinforced Polymer 4 (FRP 4), Fibre-Reinforced Polymer 5 (FRP 5), Fibre-Reinforced Polymer 6 (FRP 6) composites which can be attributed to the incorporation

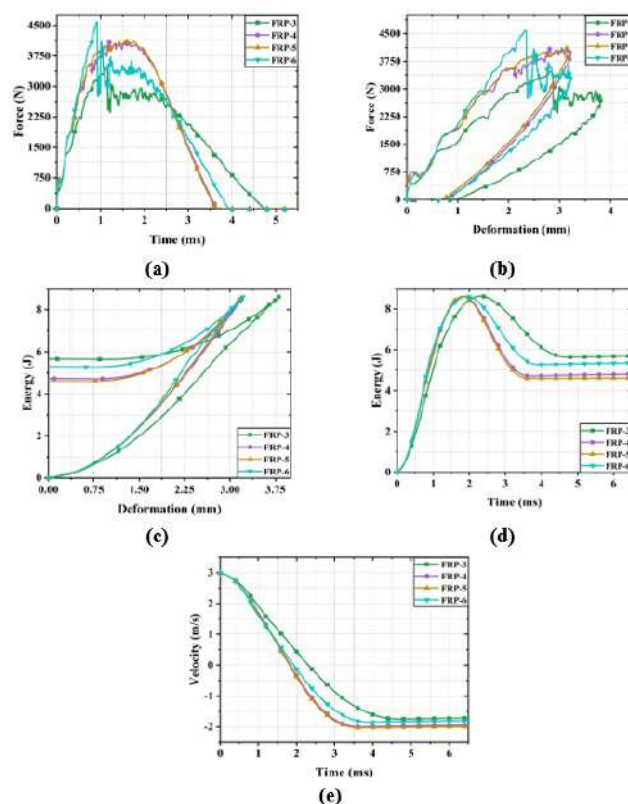


FIGURE 14. Various parameters measured during the LVI test of 40 μ SiO₂ reinforced intra-interply composites (a) Force Vs Time (b) Force Vs Deformation (c) Energy Vs Deformation (d) Energy Vs Time (e) Velocity Vs Time

of 40 μ SiO₂ particles, generally the incorporation of 40 μ SiO₂ particles impedes crack growth and also

TABLE 4. Peak Force versus Time

	Maximum Force N	Time (s)	% of improvement in maximum force due to the addition of nano silica particles
Fibre-Reinforced Polymer 3 (FRP 3)	3476.45	1.13	
Fibre-Reinforced Polymer 4 (FRP 4)	4110.98	1.41	18.25
Fibre-Reinforced Polymer 5 (FRP 5)	4113.43	1.56	18.32
Fibre-Reinforced Polymer 6 (FRP 6)	4583.81	0.91	31.85

TABLE 5. Maximum Deformation versus Force

	Maximum Deformation (mm)	Force (N)
Fibre-Reinforced Polymer 3 (FRP 3)	3.80	2660.62
Fibre-Reinforced Polymer 4 (FRP 4)	3.22	3995.83
Fibre-Reinforced Polymer 5 (FRP 5)	3.18	4054.63
Fibre-Reinforced Polymer 6 (FRP 6)	3.21	3198.38

TABLE 6. Maximum Deformation versus Time

	Maximum Deformation(mm)	Time (s)
Fibre-Reinforced Polymer 3 (FRP 3)	3.80	2.31
Fibre-Reinforced Polymer 4 (FRP 4)	3.22	1.83
Fibre-Reinforced Polymer 5 (FRP 5)	3.18	1.81
Fibre-Reinforced Polymer 6 (FRP 6)	3.21	1.92

TABLE 7. Absorbed Energy and Elastic Energy

	Total Energy (J)	Absorbed Energy (J)	Elastic Energy (J)
Fibre-Reinforced Polymer 3 (FRP 3)	8.625997	5.661351	2.95986
Fibre-Reinforced Polymer 4 (FRP 4)	8.6149	4.76184	3.85306
Fibre-Reinforced Polymer 5 (FRP 5)	8.614187	4.616976	3.997211
Fibre-Reinforced Polymer 6 (FRP 6)	8.614766	5.313688	3.301078

increases the bonding between the epoxy matrix and the reinforced elements. By the incorporation of 40 μ SiO₂ particles, the load bearing ability of Fibre-Reinforced Polymer 4 (FRP 4), Fibre-Reinforced Polymer 5 (FRP 5), Fibre-Reinforced Polymer 6 (FRP 6) increases by 18.25 %, 18.32 % and 31.85 % respectively.

Further from Figure 14 (a) and Figure 14 (b), it can be observed that even though peak load is higher for Fibre-Reinforced Polymer 6 (FRP 6), a sudden drop in load is observed after reaching the peak load. This can be attributed to the brittle mode of failure of the Fibre-Reinforced Polymer 6 (FRP 6) compos-

ite. Sudden drop in load is not observed in Fibre-Reinforced Polymer 4 (FRP 4) and Fibre-Reinforced Polymer 5 (FRP 5) due to the ductile response of the composite.

By observing Figure 14 (b) Force versus Deformation and Table 5, it can be identified that the incorporation of nano particles in the composites leads to the reduction in the deformation of the composite from 3.80 mm to 3.21 mm. This can be attributed to the stiffening of the composite laminates due to the addition of 40 μ SiO₂ particles.

By comparing the Figure 14 (a) Force versus Time, Figure 14 (b) Force Vs Deformation and

Table 5 Maximum Deformation Vs Force, it can be stated the force observed for Fibre-Reinforced Polymer 6 (FRP 6) during the maximum deformation is relatively lower when compared with the peak force of Fibre-Reinforced Polymer 6 (FRP 6) by a value of about 30.46 %, this clearly indicates, Fibre-Reinforced Polymer 6 (FRP 6) has suffered catastrophic failure. Whereas for Fibre-Reinforced Polymer 4 (FRP 4) and Fibre-Reinforced Polymer 5 (FRP 5) the drop in force at maximum deformation is about 2.80 % and 1.42 % respectively, this indicates Fibre-Reinforced Polymer 4 (FRP 4) and Fibre-Reinforced Polymer 5 (FRP 5) are stable in handling impact load unlike Fibre-Reinforced Polymer 6 (FRP 6).

Table 5 reveals that the drop in force by Fibre-Reinforced Polymer 3 (FRP 3) at maximum deformation is 23.46 % when compared with peak force exhibited by Fibre-Reinforced Polymer 3 (FRP 3), and this indicates Fibre-Reinforced Polymer 3 (FRP 3) is not that much stable in handling impact load. The absorbed energy and elastic energy were calculated from Figure 15 (d) Energy versus Time, as suggested by Volnei Tita et al. (2008) and is shown in Table 7. In general, the energy dissipation during a low velocity impact takes place in the following manner (i) Absorbed energy (ii) Elastic energy. It can be assessed that those materials with higher absorbed energy may be regarded as failed materials as they will not support the impact load due to the damage in the component. Materials which have got higher elastic energy may be regarded as useful material for impact loading due to the fact that there may be less damage. In this case Fibre-Reinforced Polymer 4 (FRP 4) and Fibre-Reinforced Polymer 5 (FRP 5) are better composites for handling impact load as they exhibit higher elastic energy.

7.1. Damage Assessment by Macroscopic Analysis by using Image J Software

The damaged assessment LVI impacted specimens of FRP 3, FRP4, FRP 5 and FRP 6 was carried out by Image J software, the damaged areas in the composites are shown in the Figures 15 (a-d) and the damage area measured through Image J software for the frontal and rear sides of the various composites is shown in the Table 8.

From the Table 8 it can be stated that the damage in Fibre-Reinforced Polymer 3 (FRP 3), on the

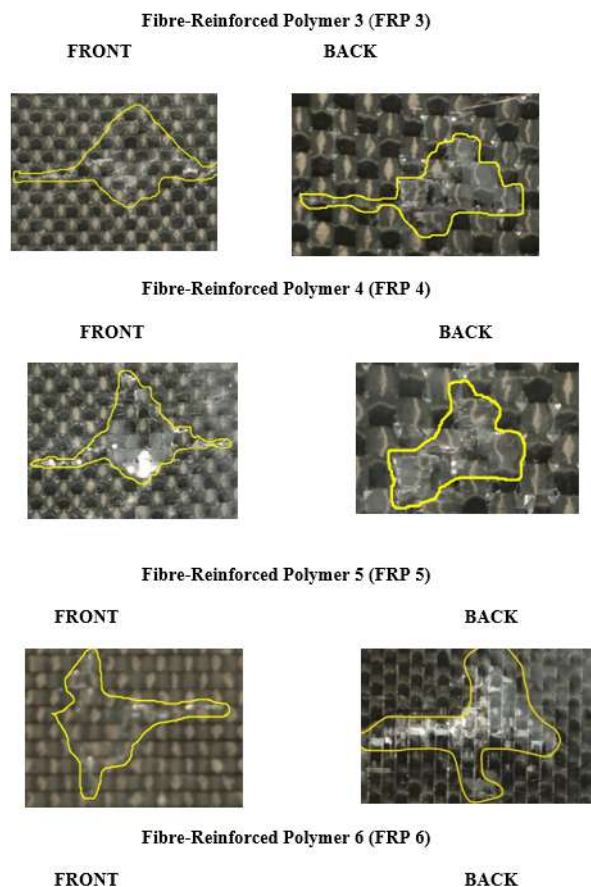


FIGURE 15. (a-h) The front and rear damaged surfaces of the low velocity impacted specimens

frontal side is 136.20 mm² and the damage area on the rear side is 26169.22 mm². The damage in Fibre-Reinforced Polymer 3 (FRP 3) on frontal and rear side is higher when compared with any other composite considered in the study. The higher damage in the Fibre-Reinforced Polymer 3 (FRP 3) can be attributed to the drastic drop in force between peak force and the force exhibited by the composite during maximum deformation. Drastic difference is an index of inability of the composite to handle impact load and the damage is spread over a large area.

From the Table 8 it can be ascertained that the damaged area in the Fibre-Reinforced Polymer 4 (FRP 4) and Fibre-Reinforced Polymer 5 (FRP 5) is comparatively lower when compared with the damage experienced by Fibre-Reinforced Polymer 3 (FRP 3), besides this Fibre-Reinforced Polymer 4 (FRP 4) and Fibre-Reinforced Polymer 5 (FRP 5) are stable in handling impact load as drastic drop in force is not observed between peak force and

TABLE 8. Damaged area in the various composites measured by Image J Software

	Damage area on the front side mm ²	Damage area on the rear side mm ²
Fibre-Reinforced Polymer 3 (FRP 3)	136.20	26169.22
Fibre-Reinforced Polymer 4 (FRP 4)	79.73	27.11
Fibre-Reinforced Polymer 5 (FRP 5)	131.92	152.68
Fibre-Reinforced Polymer 6 (FRP 6)	82.06	174.16

force experienced by the composite during maximum deformation.

Although the damage in Fibre-Reinforced Polymer 6 (FRP 6) is lower when compared with Fibre-Reinforced Polymer 3 (FRP 3), Fibre-Reinforced Polymer 6 (FRP 6) will not be a better candidate to bear impact load as drastic drop in force between peak force and the force exhibited by Fibre-Reinforced Polymer 6 (FRP 6) during maximum deformation.

7.2. Damage Assessment by Macroscopic Analysis by using Digital Microscope

The damage assessed by digital microscope for the various impacted specimens is shown Figure 16 (a-d)

The analysis of the macroscopic images by using digital microscope for Fibre-Reinforced Polymer 3 (FRP 3) shows the presence of defects like fibre breakage, matrix damage and delamination on the frontal side and distributed damage on the rear side. Whereas matrix crack, matrix failure and fibre delamination, fibre breakage and transverse crack are observed for Fibre-Reinforced Polymer 4 (FRP 4) composite. Failures such as fibre delamination, fibre breakage and matrix damage are observed in Fibre-Reinforced Polymer 5 (FRP 5) composites, the microscopic images confirm larger scale of damages in Fibre-Reinforced Polymer 5 (FRP 5) when compared with Fibre-Reinforced Polymer 4 (FRP 4). Failures such as larger cracks, fibre breakage and fibre delamination are observed in Fibre-Reinforced Polymer 6 (FRP 6) specimen.

8. Conclusion

In this work the flexural, compressive, ILSS and low velocity impact properties were studied for the various composites considered in the study. The most noticeable findings of the work are summarized. The incorporation of 40 μ SiO₂ particles up to 3 weight % improves flexural strength and

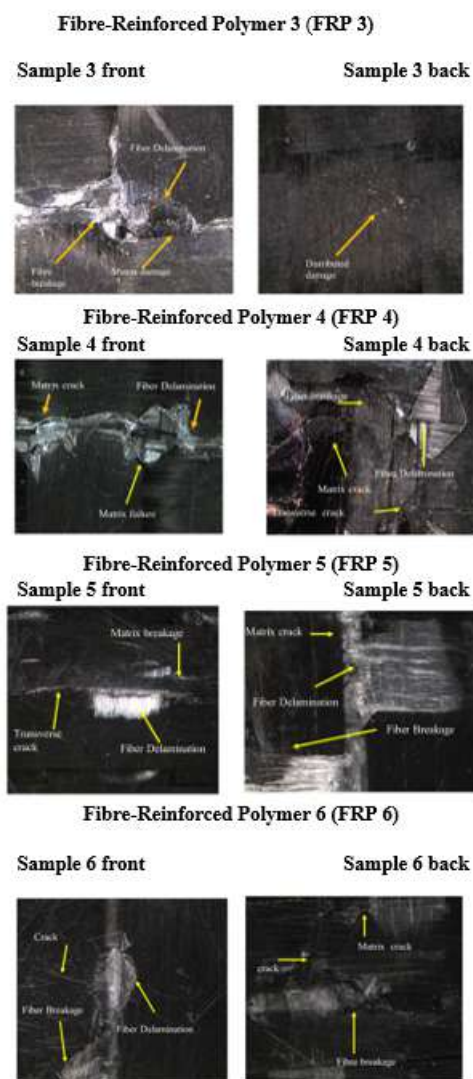


FIGURE 16. (a-d) The damage assessed by digital microscope for the various impacted specimens

compressive strength by 12 % and 23.6 %. When the incorporation exceeds 3 weight %, the flexural and compressive properties are found to decrease due to the agglomeration of 40 μ SiO₂ particles. The interlaminar shear strength is insignificant to the incorporation of 40 μ SiO₂. The incorporation of 40 μ SiO₂ particles enhances the composites rein-

forced with carbon, E-glass and parallel oriented sunn hemp fibre. For the composites reinforced with 1 weight% and 2 weight % $40 \mu \text{SiO}_2$ particles lesser variation observed is observed between the peak force and force at maximum deformation exhibited by the composites under impact load and they also exhibit higher elastic energy. This confirms the composites reinforced with 1 weight % and 2 weight % $40 \mu \text{SiO}_2$ particles will be better candidates for bearing the impact load. The damage assessment done through Image J software and digital microscopy further confirms lesser level of damage in the composites reinforced with 1 weight % and 2 weight % $40 \mu \text{SiO}_2$ particles. The aesthetic look is considered as the primary requirement for the console and the interior in the passenger cars hence the synthetic fibres are predominantly employed for this purpose. The outcome of this research work provides an alternative to the composite material made from synthetic fibres without compromising its functional requirements and aesthetic looks with eco friendliness.

References

- Akampunguza, Obed, et al. "Review of the applications of biocomposites in the automotive industry". *Polymer Composites* 38.11 (2017): 2553–2569. [10.1002/pc.23847](https://doi.org/10.1002/pc.23847).
- Das, Diptikanta, et al. "Mechanical properties and abrasion behaviour of glass fiber reinforced polymer composites – A case study". *Materials Today: Proceedings* 19 (2019): 506–511. [10.1016/j.matpr.2019.07.644](https://doi.org/10.1016/j.matpr.2019.07.644).
- Dong. "Uncertainties in flexural strength of carbon/glass fibre reinforced hybrid epoxy composites". *Composites Part B: Engineering* 98 (2016): 176–181. [10.1016/j.compositesb.2016.05.035](https://doi.org/10.1016/j.compositesb.2016.05.035).
- Manral, Ankit, Furkan Ahmad, and Vijay Chaudhary. "Static and dynamic mechanical properties of PLA bio-composite with hybrid reinforcement of flax and jute". *Materials Today: Proceedings* 25 (2020): 577–580. [10.1016/j.matpr.2019.07.240](https://doi.org/10.1016/j.matpr.2019.07.240).
- Mohan, T. P. and K. Kanny. "Compressive characteristics of unmodified and nanoclay treated banana fiber reinforced epoxy composite cylinders". *Composites Part B: Engineering* 169 (2019): 118–125. [10.1016/j.compositesb.2019.03.071](https://doi.org/10.1016/j.compositesb.2019.03.071).
- Pegoretti, Alessandro, et al. "Intraply and interply hybrid composites based on E-glass and poly(vinyl alcohol) woven fabrics: tensile and impact properties". *Polymer International* 53.9 (2004): 1290–1297. [10.1002/pi.1514](https://doi.org/10.1002/pi.1514).
- Rajpurohit, Ashok, et al. "Hybrid Effect in In-Plane Loading of Carbon/Glass Fibre Based Inter- and Intraply Hybrid Composites". *Journal of Composites Science* 4.1 (2020): 6–6. [10.3390/jcs4010006](https://doi.org/10.3390/jcs4010006).
- Ramu, P., C.V. Jaya Kumar, and K. Palanikumar. "Mechanical Characteristics and Terminological Behavior Study on Natural Fiber Nano reinforced Polymer Composite – A Review". *Materials Today: Proceedings* 16 (2019): 1287–1296. [10.1016/j.matpr.2019.05.226](https://doi.org/10.1016/j.matpr.2019.05.226).
- Reddy, P. Venkateshwar, et al. "Influence of fillers on mechanical properties of prosopis juliflora fiber reinforced hybrid composites". *Materials Today: Proceedings* 19 (2019): 384–387. [10.1016/j.matpr.2019.07.618](https://doi.org/10.1016/j.matpr.2019.07.618).
- Ren, Penggang and Zengping Zhang. "Hybrid effect on mechanical properties of M40-T300 carbon fiber reinforced Bisphenol A Dicyanate ester composites". (2010). [10.1002/pc.21016Citations:2017](https://doi.org/10.1002/pc.21016Citations:2017).
- Sair, S., et al. "Mechanical and thermal conductivity properties of hemp fiber reinforced polyurethane composites". *Case Studies in Construction Materials* 8 (2018): 203–212. [10.1016/j.cscm.2018.02.001](https://doi.org/10.1016/j.cscm.2018.02.001).
- Santini, Alessandro, et al. "Auto shredder residue recycling: Mechanical separation and pyrolysis". *Waste Management* 32.5 (2012): 852–858. [10.1016/j.wasman.2011.10.030](https://doi.org/10.1016/j.wasman.2011.10.030).
- Sivakandhan, C., et al. "Studies on mechanical properties of sisal and jute fiber hybrid sandwich composite". *Materials Today: Proceedings* 21 (2020): 404–407. [10.1016/j.matpr.2019.06.374](https://doi.org/10.1016/j.matpr.2019.06.374).
- Srinivasan, V. S., et al. "Evaluation of mechanical and thermal properties of banana–flax based natural fibre composite". *Materials & Design* 60 (2014): 620–627. [10.1016/j.matdes.2014.03.014](https://doi.org/10.1016/j.matdes.2014.03.014).

Tita, Volnei, Jonas de Carvalho, and Dirk Vandepitte. "Failure analysis of low velocity impact on thin composite laminates: Experimental and numerical approaches". *Composite Structures* 83.4 (2008): 413–428. [10.1016/j.compstruct.2007.06.003](https://doi.org/10.1016/j.compstruct.2007.06.003).

Uzay, Çağrı, Durmuş Acer, and Necdet Geren. "Impact Strength of Interply and Intraply Hybrid Laminates Based on Carbon-Aramid/Epoxy Composites". *European Mechanical Science* 3.1 (2019): 1–5. [10.26701/ems.384440](https://doi.org/10.26701/ems.384440).

Vasudevan, A., et al. "Layer-wise damage prediction in carbon/Kevlar/S-glass/E-glass fibre reinforced epoxy hybrid composites under low-velocity impact loading using advanced 3D computed tomography". *International Journal of Crashworthiness* 25.1 (2020): 9–23. [10.1080/13588265.2018.1511234](https://doi.org/10.1080/13588265.2018.1511234).

Wielage, B., et al. "Processing of natural-fibre reinforced polymers and the resulting dynamic-mechanical properties". *Journal of Materials Processing Technology* 139.1-3 (2003): 140–146. [10.1016/s0924-0136\(03\)00195-x](https://doi.org/10.1016/s0924-0136(03)00195-x).

Zah, R., et al. "Curauá fibers in the automobile industry – a sustainability assessment". *Journal of Cleaner Production* 15.11-12 (2007): 1032–1040. [10.1016/j.jclepro.2006.05.036](https://doi.org/10.1016/j.jclepro.2006.05.036).

Zhang, Jin, et al. "Hybrid composite laminates reinforced with glass/carbon woven fabrics for lightweight load bearing structures". *Materials & Design (1980-2015)* 36 (2012): 75–80. [10.1016/j.matdes.2011.11.006](https://doi.org/10.1016/j.matdes.2011.11.006).



© M. Bharathi et al. 2022 Open Access. This article is distributed under the terms of the Creative Commons Attribution 4.0 International License (<http://creativecommons.org/licenses/by/4.0/>), which permits unrestricted use, distribution, and reproduction in any medium, provided you give appropriate credit to the original author(s) and the source, provide a link to the Creative Commons license, and indicate if changes were made.

Embargo period: The article has no embargo period.

To cite this Article: Bharathi, M, S Senthil Kumaran, and P Edwin Samson. "Influence of Nano Silica Particles on Quasistatic Mechanical and Low Velocity Impact Properties of Carbon-Glass-Sunn Hemp/Epoxy in Intra-Inter Ply Hybrid Composites." *International Research Journal on Advanced Science Hub* 04.05 May (2022): 120–133. <http://dx.doi.org/10.47392/irjash.2022.032>